The Astrophysical Journal Supplement Series, 208:12 (5pp), 2013 September doi:10.1088/0067-0049/208/1/12
© 2013. The American Astronomical Society. All rights reserved. Printed in the U.S.A.

ERRATUM: "A REVISED EFFECTIVE TEMPERATURE SCALE FOR THE KEPLER INPUT CATALOG" (2012, ApJS, 199, 30)

Marc H. Pinsonneault[1], Deokkeun An[2], Joanna Molenda-Żakowicz[3], William J. Chaplin[4], Travis S. Metcalfe[5], and Hans Bruntt[6]
[1] Department of Astronomy, Ohio State University, Columbus, OH 43210, USA
[2] Department of Science Education, Ewha Womans University, Seoul 120-750, Korea; deokkeun@ewha.ac.kr
[3] Astronomical Institute, University of Wrocław, ul. Kopernika 11, 51-622 Wrocław, Poland
[4] School of Physics and Astronomy, University of Birmingham, Edgbaston, Birmingham, B15 2TT, UK
[5] Space Science Institute, 4750 Walnut Street Suite 205, Boulder, CO 80301, USA
[6] Department of Physics and Astronomy, Aarhus University, DK-8000 Aarhus C, Denmark
Received 2013 May 15; published 2013 September 4

Online-only material: color figures, machine-readable table

1. SIGN ERRORS IN THE GRAVITY CORRECTIONS

We derived surface gravity corrections to the color–temperature relationships for red giants. This step was required because we adopted a dwarf-based color calibration, and the theoretical correction is given in Figure 8. However, the sign of the correction was reversed in the note at the bottom of Table 4. In Table 7 the sense in which the corrections should have been applied is noted correctly, but the actual corrections used were reversed. In addition, null values (−999) in the gravity correction table were accidentally included in the interpolation by the sign flip error, which resulted in unreasonably large correction terms at the very cool end ($T_{\rm eff} \lesssim 4200$ K).

We have revised the data in Tables 4 and 7 accordingly, and updated the figures (Figures 8 and 18) and statistical properties (Table 8) that were impacted. Gravity terms were applied for stars with low gravities ($\log g \leqslant 3.5$), to correct for differences between the Kepler Input Catalog (KIC) and the model $\log g$ values. The $T_{\rm eff}$ estimates for dwarfs with $\log g > 3.5$ remain valid in the published version of Table 7.

A revised version of the gravity corrections is found in Table 4, with the same form and content as in the original table, except its signs. Here, $\log g$(YREC) is the $\log g$ in our YREC model (third column in Table 4). Negative values in the table mean that giants

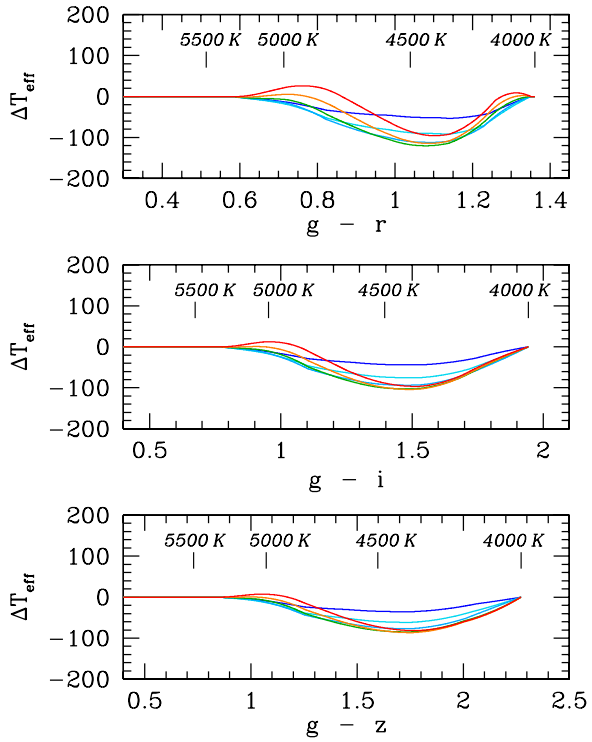

Figure 8. Theoretical $T_{\rm eff}$ corrections for various $\Delta \log g$ values with respect to the fiducial isochrones. Corrections from $\Delta \log g = 0.5$ (blue) to $\Delta \log g = 3.0$ (red) with a 0.5 dex increment are shown. The sense is that giants tend to have lower $T_{\rm eff}$ than dwarfs at fixed colors. A linear ramp was used to define smoothly varying $\Delta T_{\rm eff}$ over 4800 K $< T_{\rm eff} <$ 5800 K. In this revision, a simple quadratic relation is used to extend theoretical $T_{\rm eff}$ corrections to the very cool end ($g - r \gtrsim 1.25$), where the correction factors become zero at $T_{\rm eff} \sim 4000$ K. Only a minor fraction of giants in the sample (∼400 stars) are affected by this change.

(A color version of this figure is available in the online journal.)

Table 4
Gravity Corrections

$g-r$	$g-i/g-z$	$\log g$[a] (YREC)	$\log g$(star) − $\log g$(YREC)					
			−0.5	−1.0	−1.5	−2.0	−2.5	−3.0
$\Delta T_{\rm eff}$ when $T_{\rm eff}$ are estimated from $g-r$								
0.500	...	4.57	0.0	0.0	0.0	0.0	0.0	0.0
0.550	...	4.59	0.0	0.0	0.0	0.0	0.0	0.0
0.600	...	4.61	−1.5	−2.2	−2.3	−2.0	−1.2	0.2
0.650	...	4.62	−5.8	−8.1	−7.3	−4.5	0.2	7.2
0.700	...	4.63	−11.2	−15.3	−12.9	−6.1	4.4	18.5
0.750	...	4.64	−18.4	−26.6	−24.5	−13.8	3.8	25.7
0.800	...	4.65	−28.2	−43.2	−44.3	−31.6	−7.3	22.8
0.850	...	4.65	−36.2	−58.6	−65.1	−55.1	−29.0	6.6
0.900	...	4.66	−41.2	−69.3	−81.0	−76.3	−54.2	−18.9
0.950	...	4.66	−44.6	−77.2	−93.6	−94.7	−78.4	−45.1
1.000	...	4.67	−47.1	−83.4	−103.8	−109.3	−97.9	−69.8
1.050	...	4.67	−50.6	−88.9	−110.8	−118.8	−111.4	−88.2
1.100	...	4.68	−51.5	−90.4	−111.8	−119.4	−114.0	−95.5
1.150	...	4.69	−53.1	−90.2	−106.5	−109.9	−104.2	−88.6
1.200	...	4.69	−48.4	−80.0	−87.8	−83.8	−75.8	−61.8
1.250	...	4.70	−38.4	−56.8	−55.0	−44.8	−32.7	−18.7
1.300	...	4.72	−17.5	−25.9	−21.6	−13.0	−2.7	7.8
1.350	...	4.73	0.0	0.0	0.0	0.0	0.0	0.0
$\Delta T_{\rm eff}$ from $g-i$								
0.500	0.655	4.57	0.0	0.0	0.0	0.0	0.0	0.0
0.550	0.725	4.59	0.0	0.0	0.0	0.0	0.0	0.0
0.600	0.795	4.61	−1.2	−1.8	−1.8	−1.4	−0.6	0.5
0.650	0.865	4.62	−5.2	−7.5	−6.5	−4.0	0.2	5.9
0.700	0.934	4.63	−10.3	−14.6	−13.3	−8.3	0.3	12.0
0.750	1.003	4.64	−16.9	−25.2	−25.8	−19.4	−7.0	10.3
0.800	1.071	4.65	−24.7	−38.7	−43.5	−37.4	−22.5	−0.9
0.850	1.138	4.65	−31.1	−50.8	−60.1	−57.1	−43.4	−21.5
0.900	1.205	4.66	−34.9	−58.6	−71.4	−72.3	−61.9	−42.8
0.950	1.272	4.66	−37.9	−65.1	−80.7	−85.2	−78.6	−63.0
1.000	1.341	4.67	−41.3	−70.9	−88.3	−95.3	−92.0	−79.2
1.050	1.411	4.67	−43.4	−74.3	−92.5	−101.1	−100.6	−90.4
1.100	1.483	4.68	−43.8	−75.3	−93.6	−102.7	−103.9	−95.9
1.150	1.559	4.69	−43.1	−73.7	−90.8	−98.7	−100.4	−94.2
1.200	1.639	4.69	−38.3	−66.2	−80.6	−85.9	−86.7	−82.0
1.250	1.724	4.70	−29.8	−52.7	−63.0	−63.2	−62.4	−58.5
1.300	1.816	4.72	−16.1	−31.1	−38.2	−34.7	−34.0	−30.9
1.350	1.920	4.73	−2.6	−6.0	−7.6	−6.1	−6.0	−5.2
$\Delta T_{\rm eff}$ from $g-z$								
0.500	0.708	4.57	0.0	0.0	0.0	0.0	0.0	0.0
0.550	0.795	4.59	0.0	0.0	0.0	0.0	0.0	0.0
0.600	0.881	4.61	−0.8	−1.2	−1.1	−0.9	−0.4	0.4
0.650	0.966	4.62	−3.6	−5.1	−4.4	−2.5	0.3	4.4
0.700	1.050	4.63	−7.7	−11.2	−10.1	−6.3	−0.6	7.5
0.750	1.133	4.64	−13.5	−20.6	−20.7	−15.6	−7.5	4.2
0.800	1.215	4.65	−20.4	−32.5	−35.5	−30.7	−21.1	−6.5
0.850	1.294	4.65	−25.5	−41.7	−48.3	−46.4	−37.3	−22.4
0.900	1.373	4.66	−28.1	−47.0	−56.6	−58.3	−50.9	−37.5
0.950	1.452	4.66	−30.2	−51.6	−63.9	−68.4	−63.3	−51.8
1.000	1.533	4.67	−33.0	−56.5	−70.5	−76.7	−74.0	−64.3
1.050	1.616	4.67	−34.8	−59.9	−74.9	−82.2	−81.7	−73.9
1.100	1.703	4.68	−35.4	−61.3	−76.7	−84.6	−85.9	−80.0
1.150	1.794	4.69	−34.6	−60.1	−75.3	−83.2	−85.5	−81.3
1.200	1.891	4.69	−30.3	−53.7	−67.8	−74.9	−77.6	−75.2
1.250	1.995	4.70	−22.7	−42.1	−54.2	−59.5	−61.8	−61.0
1.300	2.110	4.72	−13.0	−25.9	−32.0	−40.3	−42.2	−41.6
1.350	2.241	4.73	−2.6	−5.3	−6.1	−8.9	−9.3	−9.2

Notes. In the published version of Table 4, gravity corrections had sign flip errors. $\Delta T_{\rm eff}$ values should be added to dwarf-based $T_{\rm eff}$ estimates, if one wishes to infer $T_{\rm eff}$ for giants or subgiants.

[a] The $\log g$ values in the base isochrone (Table 1 of the published version of this article).

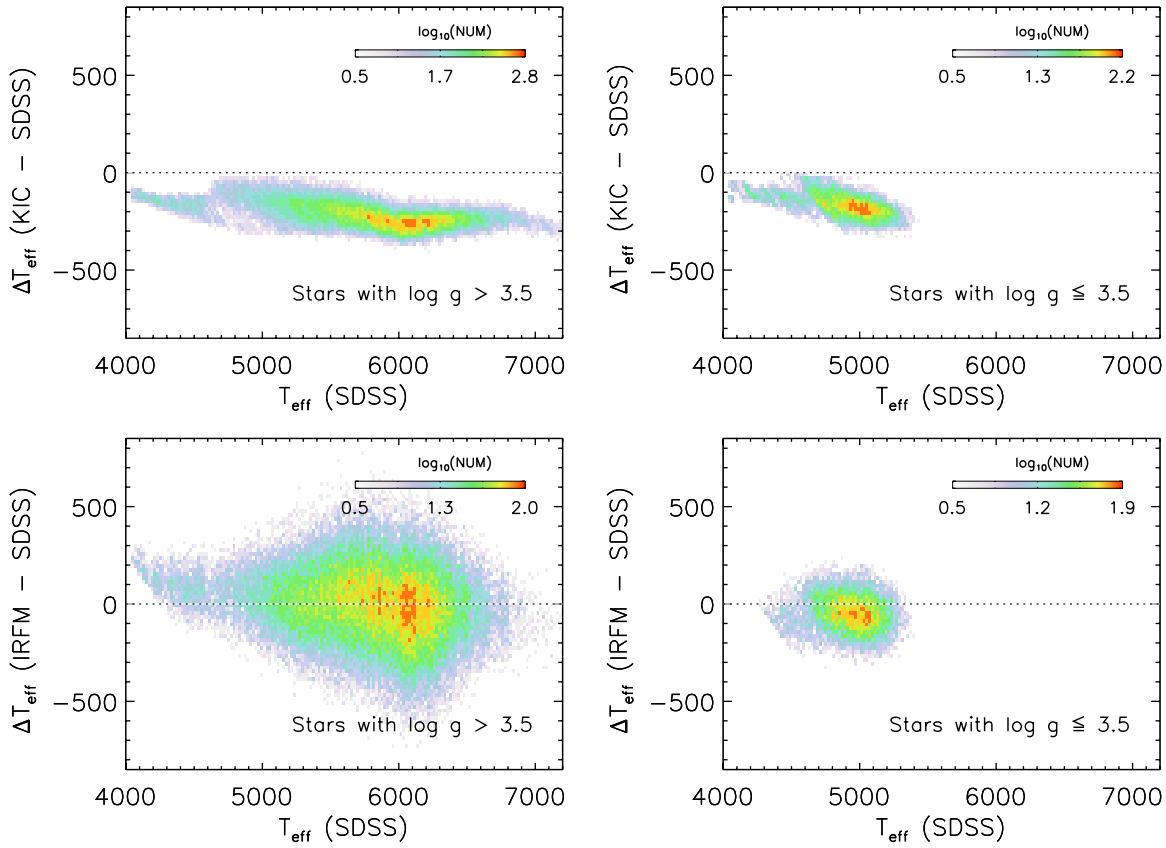

Figure 18. Comparisons of $T_{\rm eff}$ using the final SDSS $T_{\rm eff}$ estimates. Comparisons are shown for the original KIC $T_{\rm eff}$ for dwarfs (top left) and giants (top right), and for the $(J - K_s)$-based IRFM estimates for dwarfs (bottom left) and giants (bottom right). The comparisons for giants shown in the panels on the right are affected by the sign flip errors in the gravity corrections described in this erratum. The comparisons for dwarfs in the panels on the left are unaffected and are the same as in the published version of this article.

(A color version of this figure is available in the online journal.)

Table 7
Catalog with Revised $T_{\rm eff}$

KIC_ID	SDSS			IRFM[a]			KIC				
	$T_{\rm eff}$ (K)	$\sigma_{\rm tot}$ (K)	$\sigma_{\rm ran}$ (K)	$T_{\rm eff}$ (K)	$\sigma_{\rm tot}$ (K)	$\sigma_{\rm ran}$ (K)	$T_{\rm eff}$ (K)	$\log g$ (dex)	[Fe/H] (dex)	$\Delta T_{\rm eff}$[b] (K)	Flag[c]
757076	5137	85	55	5150	98	94	5174	3.60	−0.08	0	0
757099	5523	97	34	5270	110	101	5589	3.82	−0.21	0	0
757137	4724	74	42	4536	101	99	4879	2.58	−0.08	−49	0
757218	4594	79	17	4489	90	75	4555	2.28	−0.12	−67	0
757231	4861	116	64	4974	111	89	4825	2.60	−0.08	−24	0

Notes. In the published version of Table 7, there were sign flip errors in the gravity corrections ($\Delta T_{\rm eff}$), which affected the SDSS $T_{\rm eff}$ for giants ($\log g \leqslant 3.5$). The other columns are unaffected. We have revised the gravity corrections so that they are now properly applied. Effective temperatures presented here were computed at a fixed [Fe/H] = −0.2.

[a] IRFM $T_{\rm eff}$ estimates based on $J - K_s$.

[b] $T_{\rm eff}$ correction for giants. The correction factor has already been applied to the SDSS $T_{\rm eff}$ estimate in the second column of the above table.

[c] Quality flag indicating stars with unusually discrepant SDSS $T_{\rm eff}$ estimates (Flag = 1). See Section 4.2.4 for details.

(This table is available in its entirety in a machine-readable form in the online journal. A portion is shown here for guidance regarding its form and content.)

have lower $T_{\rm eff}$ than dwarfs at fixed colors. Therefore, $\Delta T_{\rm eff}$ values in Table 4 should be added to dwarf-based $T_{\rm eff}$ estimates if one wishes to infer $T_{\rm eff}$ for giants or subgiants.

We also revised our scheme to handle the gravity corrections in the very cool end ($T_{\rm eff} \lesssim 4200$ K). A revised plot of the gravity corrections is presented in Figure 8. In the new procedure, a simple quadratic relation was used to generate a smooth transition to a zero correction term at $T_{\rm eff} \sim 4000$ K for the color–temperature relationship, which is the place where dwarf and giant relations cross in Figure 7. Only a minor fraction of stars in our sample (∼400 giants) are affected by this change.

Table 8
Statistical Properties of $T_{\rm eff}$

$\langle T_{\rm eff}\rangle$	$\langle(g-r)_0\rangle$	$N_{\rm stars}$	IRFM − KIC[a]			SDSS − KIC[a]			SDSS − IRFM[a]			$T_{\rm eff}$(color) − $T_{\rm eff}$(*griz*)			SDSS	
(KIC)			$\Delta T_{\rm eff}$	σ	$\sigma_{\rm prop}$	$\Delta T_{\rm eff}$	σ	$\sigma_{\rm prop}$	$\Delta T_{\rm eff}$	σ	$\sigma_{\rm prop}$	$g-r$	$g-i$	$g-z$	σ_{griz}[b]	$\sigma_{\rm prop}$[c]
Giants (KIC $\log g \leqslant 3.5$)																
5292	0.51	35	246	204	122	216	38	35	−62	198	132	−5	−4	29	34	29
5184	0.56	175	167	111	112	214	41	35	30	132	121	−31	−1	37	39	27
5086	0.60	676	159	100	108	215	45	34	36	104	117	−32	0	35	37	25
4995	0.65	2098	135	99	105	208	45	33	50	106	113	−38	1	36	38	23
4897	0.69	3376	129	96	101	207	44	32	52	103	110	−38	1	35	37	21
4800	0.74	4316	124	91	98	202	46	30	48	99	105	−38	1	36	36	19
4702	0.79	3435	118	91	94	192	51	27	39	101	101	−37	0	37	34	17
4599	0.85	3002	110	95	91	178	56	24	36	108	96	−30	−2	34	28	16
4509	0.91	1148	71	106	87	151	53	20	56	118	91	−25	−3	32	23	14
4401	0.97	930	58	97	84	148	46	17	75	109	87	−19	−5	29	18	13
4307	1.03	861	64	80	81	138	41	16	62	88	84	−16	−6	27	16	12
4202	1.10	665	97	53	79	123	32	14	20	60	81	−3	−7	19	13	12
4105	1.20	631	169	29	80	103	28	14	−60	33	83	22	−7	3	15	11

Notes. We only present statistical properties for giants (KIC $\log g \leqslant 3.5$) in this table. The results for dwarfs (KIC $\log g > 3.5$) are the same as in the published version of Table 8. The statistical properties derived from the full long-cadence sample included the corrections to the temperature scale at the hot end as described in the text and the gravity corrections for giants. No metallicity and binary corrections were applied.

[a] The weighted mean difference ($T_{\rm eff}$), weighted standard deviation (σ), and the expected standard deviation propagated from random errors ($\sigma_{\rm prop}$).

[b] The median of the standard deviation, which is derived from individual $T_{\rm eff}$ estimates in $g-r$, $g-i$, and $g-z$ for each star.

[c] The median of the standard deviation, which is propagated from photometric errors in *griz* for each star.

A revised main catalog (Table 7) shows Sloan Digital Sky Survey (SDSS) $T_{\rm eff}$ estimates after correcting for the difference in gravity at $\log g$(KIC) $\leqslant 3.5$. For giants the mean and median changes from the original version are 59 K and 36 K, respectively, at $T_{\rm eff} > 4200$ K. The dwarf-based solution can be obtained by subtracting the tabulated correction terms ($\Delta T_{\rm eff}$) in Table 7.

Figure 18 is a replacement for the published figure and shows comparisons of our revised $T_{\rm eff}$ with those of the KIC (top panels) and Infrared Flux Method (IRFM; bottom panels). Comparisons for dwarfs in the left panels are unaffected by the sign flips in the gravity corrections. However, an improved agreement is seen between the IRFM and SDSS (YREC) scales for red giants (lower right panel). The discrepancy with the original KIC remains, but the differences for cool giants are significantly smaller.

The corrected statistical properties of the temperature differences between SDSS, IRFM, and KIC estimates are shown in Table 8, a replacement for the published table. For hotter giants the differences from prior results are zero, while the magnitude of the error rises to 210 K at the cool end of the calibration range. The weighted mean differences for giants are −165 K (a median difference of −161 K) for the KIC minus SDSS temperatures and −47 K (a median difference of −42 K) for the IRFM minus SDSS temperatures. The differences were −252 K (median −215 K) and −109 K (median −92 K), respectively, from prior results. A significant offset between the KIC and SDSS values remains, which is one of our main results in the paper.

The main focus of the published paper concerned the $T_{\rm eff}$ scale for dwarfs, which is not impacted. With the revised $\log g$ corrections, a smaller number of stars (5,347 versus 5,798 among 154,931 stars with a valid SDSS $T_{\rm eff}$) are now flagged as having internally inconsistent $T_{\rm eff}$ estimates, according to our quality criteria (see Section 4.2.4 of the published version of this article). Comparisons of the revised $T_{\rm eff}$ for giants with spectroscopic samples in Figure 14 are unaffected, as the gravity corrections have correctly been applied in this case.

2. DETAILED STEPS TO COMPUTE MEAN $T_{\rm eff}$ AND ITS ERRORS

Regardless of the sign flip errors in the gravity corrections, we provide below detailed descriptions on how to obtain mean $T_{\rm eff}$ and its random and systematic errors using YREC isochrones in *griz* passbands.

The mean $T_{\rm eff}$ can be determined in the following way. This complements a description in the third step of "A Recipe for Estimating $T_{\rm eff}$" in Section 4.1 of the published paper. For a given set of *griz* magnitudes, which were corrected for the photometry zero-point errors and interstellar extinctions in the previous steps, one can determine a mean distance modulus for each star using model magnitudes in *griz*:

$$(m - M)_0 = \frac{\Sigma_i \left[(m_{{\rm obs},i} - m_{{\rm model},i})/\sigma_i^2\right]}{\Sigma_i \left(1/\sigma_i^2\right)}, \quad (1)$$

where the subscript i indicates each of the *griz* passbands. The $m_{{\rm obs},i}$ and σ_i are observed magnitude and its error (0.01 mag in *gri* and 0.03 mag in z) in each passband. The $m_{{\rm model},i}$ is the model magnitude in each passband from our base isochrone in Table 1.

From this, one can compute a χ^2 value of the model fit for each star as follows:

$$\chi^2 = \Sigma_i \frac{[(m_{{\rm obs},i} - m_{{\rm model},i}) - (m - M)_0]^2}{\sigma_i^2}. \quad (2)$$

We searched for a minimum χ^2 of the model fit in the entire mass grid of our base isochrone, and determined a mean $T_{\rm eff}$ as the one that gives the most consistent fit overall to the data in *griz* passbands. The best-fitting $T_{\rm eff}$ is shown in the second column in Table 7.

Random errors in $T_{\rm eff}$ were obtained in the following way. We applied photometric errors to each passband ($\pm$0.01 mag in *gri* and $\pm$0.03 mag in *z*), and computed $T_{\rm eff}$. Taking the mean difference from the original $T_{\rm eff}$ as an effective 1σ error, we added in quadrature $T_{\rm eff}$ errors from all photometric passbands in *griz*. We also computed a random error by taking a standard deviation of individual $T_{\rm eff}$ estimates from $g - r$, $g - i$, and $g - z$, respectively. We then took a larger one from the above two approaches as the size of a representative random source of error. This error is shown in the fourth column ($\sigma_{\rm ran}$) in Table 7.

Systematic errors in $T_{\rm eff}$ were estimated as follows. For the error in the reddening, we repeated computing $T_{\rm eff}$ with 15% lower and higher $E(B - V)$ values than in the KIC, and took the mean difference from the original $T_{\rm eff}$ as an effective $\pm 1\sigma$ error. For the error from the metallicity, we computed $T_{\rm eff}$ from models at [Fe/H] $= -0.5$ and [Fe/H] $= +0.1$ (one can use our tabulated metallicity corrections in Table 3 in the published version of this article), and took the mean difference from an original $T_{\rm eff}$ as an effective $\pm 1\sigma$ error in $T_{\rm eff}$. From both errors in reddening and metallicity, we obtained a total systematic error in $T_{\rm eff}$ by adding individual errors in quadrature. Based on both random and systematic errors, the total error was computed as a quadrature sum of these errors, and is tabulated in the third column ($\sigma_{\rm tot}$) in Table 7.